Conformation of Myosin in Dilute Solution as Estimated from Hydrodynamic Properties†

Jose García de la Torre‡ and Victor A. Bloomfield*

ABSTRACT: On the basis of the current knowledge of the structure and dimensions of myosin and its parts, we analyze available data on hydrodynamic properties (translational diffusion, rotational diffusion, and intrinsic viscosity) for comparison with values calculated for models with varying geometry. Special attention is paid to detecting flexibility effects in those properties. After obtaining a plausible model for subfragment S-1, we concentrate on the conformation of the rodlike parts of myosin. Although uncertainties in the experimental values do not allow a rigorous, quantitative analysis, we show how hydrodynamic data provide evidence for the flexibility of the rod at the joint of subfragment S-2 and light meromyosin.

In Huxley's (1969) hypothesis for the mechanism of muscle contraction, the myosin molecule was assumed to be hinged at well-defined sites which are customarily identified as the points of attack of proteolytic enzymes (Lowey, 1971). According to our current knowledge of myosin, flexibility is possible at the junction of the heads (subfragment S-1) and the rod as well as within the rod, near the joint of subfragments S-2 and light meromyosin (LMM).

Much effort has been devoted to the detection of flexibility in myosin in order to check Huxley's hypothesis. In many instances the approach has been to observe the molecule in the electron microscope (EM) [Elliot & Offer (1978) and references cited therein]. Thus, Elliot & Offer (1978) have recently obtained EM pictures of myosin in which the heads adopt a variety of conformations with respect to the rod, and the rod itself is seen to be kinked near its middle point. Elliot & Offer (1978) also report on the dimension and shape of the myosin heads (S-1).

Although EM studies are excellent starting points for the characterization of the conformation of biological macromolecules, their conclusions can never be regarded as definitive, for there is always a reasonable doubt whether the macromolecule has been altered during the preparation of the EM specimen. On the other hand, hydrodynamic studies in solution yield structural information that must correspond more closely to the conformation of the macromolecule under physiological conditions. The hydrodynamic properties of myosin and its subfragments have been the subject of previous experimental research (references will be given later on in this paper), but the interpretation remained difficult because of the lack of a theoretical formalism able to predict the hydrodynamic properties of macromolecules having a complex shape. Such a formalism has now been developed by several workers (García de la Torre & Bloomfield, 1978; Nakajima & Wada, 1977; García Bernal & García de la Torre, 1980), and it is the purpose of this paper to analyze the experimental results by comparison with values computed for models of myosin and its subfragments. The theory is only valid for rigid particles, but, as we shall show later, a first-order estimate of the flexibility effects can be made. In this way we are led to the conclusion that the experimental results can only be interpreted when myosin is regarded as a hinged macromolecule. However, a quantitative description of flexibility is impossible at present owing both to inadequacies of the theory for this kind of particle and to uncertainties in the experimental results.

Methods

The first step in the calculation of hydrodynamic properties is to model the particle by using spherical elements of arbitrary radius. The shape and dimensions of the model must be as close as possible to those of the macromolecule. For subfragment S-1 we have accepted the pear-like shape proposed by Elliot & Offer (1978), and the myosin rod has been modeled as we suggested for broken rods in previous papers (García de la Torre & Bloomfield, 1978; García Bernal & García de la Torre, 1980). The reader is also referred to these papers for the description of the theoretical formalism; we will not repeat such details here. We simply point out that translation–rotation coupling has been considered due to the low symmetry of myosin, and the resulting values for translational and rotational diffusion and for intrinsic viscosity are referred to the centers of diffusion and viscosity, respectively.

In the study of the rodlike parts of myosin, we will make use of analytical expressions that give the dependence of the hydrodynamic properties of a rod of length L on the diameter, d, of the rod. These expressions are

$$D = A + B \ln (L/d) \quad (1)$$

$$1/(M_r[\eta]) = C + D' \ln (L/d) \quad (2)$$

$$D_r = E + F \ln (L/d) \quad (3)$$

where D is the translational diffusion coefficient, $[\eta]$ is the intrinsic viscosity, D_r is the rotational diffusion coefficient, and M_r is the molecular weight. A, B, C, D', E, and F are constants which depend on L and other physical properties of the macromolecule and solvent. Equations 1–3 have been known for many years for straight rods, and, as demonstrated by Wilemski (1977), they also hold for a broken rod with arms of length L_1 and L_2 ($L_1 + L_2 = L$). However, the values that early treatments predicted for the constants are somewhat in error, due to the various approximations embodied in them. Therefore, we have preferred to obtain the constants A to F for the myosin rod from numerical values calculated by using our theory.

In the case of myosin, the hydrodynamic behavior will be dominated by the rod, and the contribution from the heads

† From the Department of Biochemistry, The University of Minnesota, St. Paul, Minnesota 55108. *Received January 14, 1980.* This work was supported by National Science Foundation Grant PCM-7806777 and by a fellowship from the U.S.A.–Spain Joint Committee for Scientific and Technological Cooperation to J.G.T.

‡ Permanent address: Departamento de Quimica Fisica, Facultad de Ciencias, Universidad de Extremadura, Badajoz, Spain.

0006-2960/80/0419-5118$01.00/0

can be regarded as an end-effect correction. Then, the hydrodynamics of rodlike particles (Broersma, 1960a,b; Yoshizaki & Yamakawa, 1980) tell us that the constants A, C, and E (and perhaps B, D', and F) will be different for myosin than for the rod, but the linear relationships between the properties and ln (L/d) will still hold. Then, eq 1–3 will also be used to extrapolate the properties calculated for myosin models with varying rod diameter.

The theoretical formalism used throughout this paper (García de la Torre & Bloomfield, 1978; García Barnal & García de la Torre, 1980) is known to yield quite accurate results except in the case of rotational diffusion and intrinsic viscosities of models in which one or a few elements are not much smaller than the particle as a whole (García de la Torre & Bloomfield, 1978; Wilson & Bloomfield, 1979a). This does not happen for myosin, myosin rod, and heavy meromyosin (HMM), but some problems could arise for the models we will use for the heads (see Figure 1). For this reason, the intrinsic viscosity of the heads will be computed with the equation proposed by Tsuda (1970), which works fairly well for particles that are not too elongated.

Results

Subfragment S-1. The physical properties of myosin heads (subfragment S-1) are as follows: molecular weight M_r = 115 000 [110 000 for S-1 (A1) and 120 000 for S-1 (A2)] (Lowey et al., 1969); partial specific volume $\bar{v}$ = 0.734 cm^3/g [0.74 calculated from amino acid composition, 0.728 from density measurements (Yang & Wu, 1977)]; sedimentation coefficient $s^0_{20,w}$ = 5.8 S; translational diffusion coefficient $D^0_{20,w}$ = 4.8 × 10^{-7} cm^2/s; intrinsic viscosity $[\eta]$ = 6.4 cm^3/g; rotational diffusion coefficient D_r = 1.17 × 10^6 s^{-1} [calculated from the relaxation time of nanosecond fluorescence depolarization (Mendelson et al., 1973) and corrected to 20 °C].

A first attempt to interpret these values can be made in terms of a spherical model, as earlier proposed by Lowey et al. (1969). From M_r and $\bar{v}$ one gets a dry volume of the particle v' = 140 000 Å^3, and this gives r_u = 32 Å for the radius of the unhydrated sphere. However, the hydrodynamic radii are r_t = 45 Å from $D^0_{20,w}$, r_η = 49 Å from $[\eta]$, and r_r = 52 Å from D_r. The deviation of any of these three values from r_u suggests that S-1 in solution is nonspherical and/or hydrated. As the three hydrodynamic radii are not very different, S-1 cannot be too elongated and this in turn indicates hydration.

Yang & Wu (1977) analyzed the hydrodynamic properties of S-1 by using prolate and oblate ellipsoidal models. A combination of the two hydrodynamic properties can be made in such a way that the axial ratios of the equivalent prolate and oblate ellipsoids, p and q, are obtained independently of hydration. For a given geometry, the hydration paramter δ_1 (grams of H_2O/grams of protein) can be calculated next. The analysis of Yang and Wu gives p = 5 (δ_1 = 0.3–0.6) from $s^0_{20,w}$ and $[\eta]$, p = 1.5 (δ_1 = 1.2–1.7) or q = 4.5 (δ_1 = 0.60–0.90) from $[\eta]$ and D_r, and p = 2 (δ_1 = 1.1–1.5) or q = 9 (δ_1 = 0.05–0.10) from $s^0_{20,w}$ and D_r. The discrepancies between the several values of p, q, and δ could be due to experimental errors in the hydrodynamic properties but also may indicate that ellipsoids are not good hydrodynamic models for S-1. In any case, it can be concluded that S-1 is moderately nonspherical (p or q = 2–5) and considerably hydrated ($\delta > 0.3$).

The shape of S-1 has been investigated by Kretzschmar et al. (1978) using low-angle X-ray scattering. The radius of gyration obtained from a Guinier plot would correspond to ellipsoids with either p = 2.3 (δ_1 = 0.3) or q = 2.5 (δ_1 = 0.4), in disagreement with the hydrodynamic values, and measurements at higher angles deviated remarkably from the curves expected for prolate and oblate ellipsoids. These findings confirm that S-1 is not precisely ellipsoidal. Other peculiar shapes proposed in earlier studies, such as a short, fat cylinder (Miller & Tregear, 1972) and even a bent rod (Moore et al., 1970), seem not to be supported by more recent observations.

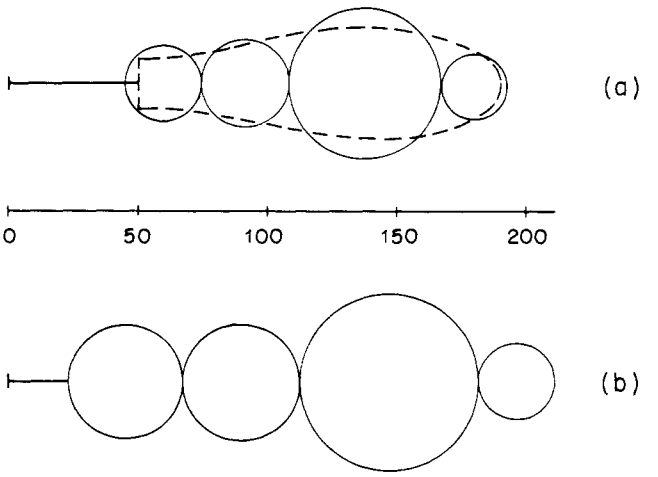

FIGURE 1: (a) Model for myosin heads based on shape and dimensions determined by Elliot & Offer (1978). The discontinuous line is the contour of their model. For hydrodynamic calculations, we have used the represented set of four spheres, which has similar shape, length, and volume. The connector is assumed to be frictionless. The horizontal axis gives distances from the head–tail joint. (b) New model after a 23% expansion to account for hydration (see text). The radii of the spheres, from left to right, are 20, 22, 34, and 14 Å. The frictionless connector is now 25 Å long.

The dimensions and shape of S-1 have been recently reexamined in the detailed electron microscopy study of Elliot & Offer (1978). They represent S-1 as a revolution body (see Figure 6 in their paper) ~150 Å long and 50 Å wide at the widest point, which is connected to the myosin tail by a thinner region that is poorly resolved. The volume of this particle turns out to be very close to the unhydrated volume of S-1. In order to calculate the hydrodynamic properties (García de la Torre & Bloomfield, 1977a,b, 1978; García Bernal & García de la Torre, 1980) of S-1 from the results of Elliot and Offer, we used a model composed by four touching spheres, whose overall shape, dimensions, and volume (132 000 Å^3) are quite similar to theirs. A frictionless connector, 50 Å long, was included in the model to represent the unresolved region. In Figure 1a our model is depicted along with Elliot and Offer's.

Owing to the axial symmetry to our model, no translational–rotation coupling occurs at the center of diffusion (García Bernal & García de la Torre, 1980), so that $D^0_{20,w}$ can be directly calculated from the translational friction tensor (García de la Torre & Bloomfield, 1977a). As noted under Methods, the equation by Tsuda (1970) was used to compute $[\eta]$. For a prolate ellipsoid of similar dimensions, this equation deviates at most 10% from the exact result (García de la Torre & Bloomfield, 1978). The procedure of Wilson & Bloomfield (1979a) could be applied to get D_r and a refined value of $[\eta]$, but the uncertainties in experimental data on which our model is based do not guarantee the success of any further computational effort. The calculated values for the model in Figure 1a are $D^0_{20,w}$ = 5.76 × 10^{-7} cm^2/s and $[\eta]$ = 2.8 cm^3/g.

These results deviate remarkably from the experimental ones. If the shape of the model is correct, then we have to assume that S-1 is bigger in solution than in the electron microscopy preparations. The large amount of hydration suggested above could well account for the expansion. If we take, for instance, δ = 0.65 as a plausible value, the ratio of

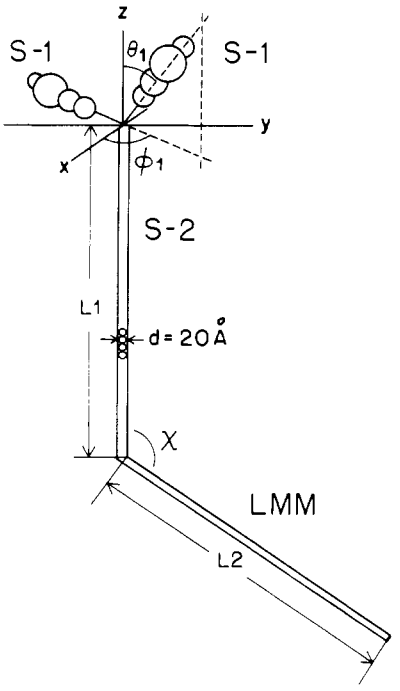

FIGURE 2: Geometry of the myosin model. The dimension and shape of the heads (S-1) are those given in Figure 1b. The rodlike portions are modeled by using 20-Å beads. The models for myosin rod and heavy meromyosin (HMM) are obtained by eliminating the two heads and the light meromyosin (LMM), respectively.

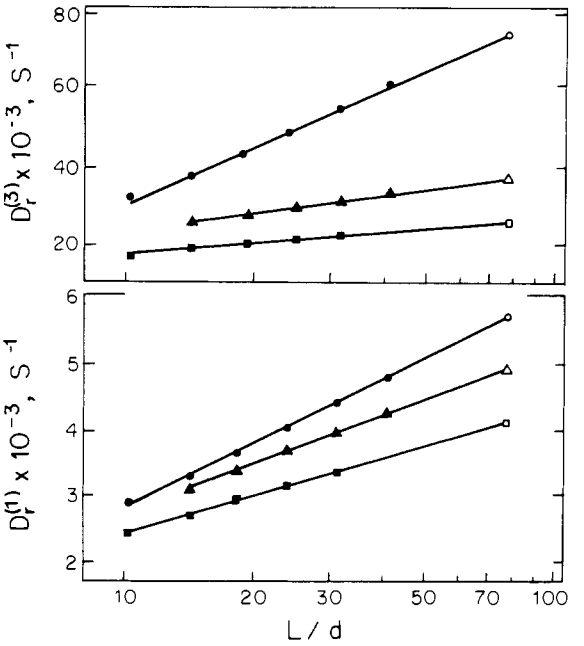

FIGURE 3: Variation of calculated translational diffusion coefficient, $D^0_{20,w}$, and intrinsic viscosity [expressed as $1/(M_r[\eta])$] with the length to diameter ratio, L/d, for L = 1560 Å and $\chi = 90°$. (Circles) Myosin rod (no heads); (triangles) myosin with $\theta_1 = 110°$, $\phi = 0°$, $\theta_2 = 110°$, and $\phi_2 = 90°$; (squares) myosin with $\theta_1 = 60°$, $\phi_0 = 90°$, $\theta_2 = 60°$, and $\phi_2 = 270°$. Closed symbols are calculated values, and the straight lines represent the corresponding linear least-squares fits. Open symbols are the values extrapolated at d = 20 Å.

hydrated to dry volume, calculated as $1 + \delta/\bar{v}$, would be 1.86. This can be accomplished by a 23% uniform expansion of the model, which leads to the dimensions represented in Figure 1b. Now the length of the frictionless connector has been reduced to 25 Å, just the right order of magnitude to prevent the distance from the top of the head to the joint from taking too large a value. The calculated properties are now $D^0_{20,w} = 4.7 \times 10^{-7}$ cm^2 s^{-1} and $[\eta] = 5.3$ cm^3/g, in better agreement with experiments.

We cannot claim any important success in the analysis of the hydrodynamic properties of S-1 since it is based on somewhat arbitrary choice for the hydration parameter, and, in fact, the agreement with experimental values is not much better than that found for ellipsoidal models (Yang & Wu, 1977). However, our model, besides being hydrodynamically acceptable, reproduces closely what is observed by electron microscopy, and we therefore think that it can be used in the subsequent calculations for myosin and heavy meromyosin.

Myosin and Myosin Rod. The two subfragments composing the myosin rod, subfragment S-2 and light meromyosin (LMM), are presumably rodlike, and, therefore, their properties can be interpreted by using the well-known equations for cylinders (Broersma, 1960a,b; Yamakawa & Fujii, 1973; Tirado & García de la Torre, 1979). Hence, we shall concentrate on the more complicated shapes of myosin, myosin rod, and heavy meromyosin (HMM).

The model for the whole myosin molecule is given in Figure 2. The myosin rod (S-2 plus LMM) lies in the $(+y, -z)$ quadrant, with S-2 on the z axis. A variable angle χ is assumed at the joint of S-2 and LMM, which are modeled as linear arrays of beads having a diameter of 20 Å. When necessary, a smaller extra bead is included to get exactly the desired length. Our choice for the diameter of the rod is based on a hydrated polypeptide α helix, and we should recall that the calculated properties are not very sensitive to it. The two heads meet the rod at the origin of the coordinates. The orientation of the heads is determined by the polar angles θ_1,ϕ_1 and θ_2,ϕ_2 of their axes. Elliot & Offer (1978) have found that the heads can adopt a variety of different positions, which indicates high flexibility in the joint of S-1 and S-2. Therefore, we have placed no restriction on the orientation of the heads, prohibiting only those configurations that show head–head or head–tail overlapping. We will denote the lengths of S-2 and LMM as L_1 and L_2, respectively, so that $L = L_1 + L_2$ is the length of the rod. The models for myosin rod and HMM are obtained by eliminating the heads and the LMM, respectively.

If d = 20 Å and L = 1560 Å, 78 elements are needed to model the rod, and 8 more are necessary for the heads in myosin. However, in the computer facilities available to us, the computational procedures of our theory were limited in practice to models with <60 elements. To circumvent this problem, we followed a strategy based on eq 1–3 and the considerations presented under Methods. For each set of values of L_1, L_2, χ, ϕ_1, θ_1, ϕ_2, and θ_2, calculations were carried out for d = 150, 110, 85, 65, 50, and 38 Å. Then the coefficients in eq 1–3 for each property were obtained by least-squares fitting from plots of the property vs. ln (L/d).

This is illustrated in Figures 3 and 4 for myosin with χ = 90° and two different conformations of the heads and for the myosin rod also with $\chi = 90°$. It is seen that the linearity is quite good; in fact, correlation coefficients >0.999 were found in these and in most other cases. For myosin the linearity was even better when $\chi = 180°$ since then the relative contribution of the heads is smaller. Hence, the least-squares straight lines can be used to extrapolate to the value of L/d that corresponds to d = 20 Å. Using this extrapolation procedure, we calculated the hydrodynamic properties of myosin and the myosin rod for $\chi = 180°$ and $\chi = 90°$ and two different geometries of the rod, with L = 1560 (L_1 = 430 Å) and 1440 Å (L_1 = 720 Å). The first set of lengths is the one suggested by Elliot & Offer (1978). These authors found that a well-defined bend appears at ~30 Å from the head end of the rod. However, their value of L is somewhat larger than those obtained in

Table I: Calculated and Experimental Hydrodynamic Properties of Myosin and Myosin Rod (20 °C)

properties	calcd values: L = 1440 Å, L_1 = 720 Å, χ = 180°	L = 1440 Å, L_1 = 720 Å, χ = 90°	L = 1560 Å, L_1 = 430 Å, χ = 180°	L = 1560 Å, L_1 = 430 Å, χ = 90°	exptl values
Myosin[a]					
$D^0_{20,w} \times 10^7$, cm² s⁻¹	1.17 (0.01)	1.19 (0.01)	1.15 (0.01)	1.17 (0.01)	1.24,[f] 1.11[g]
$[\eta]$, cm³ g⁻¹	245 (19)	162 (18)	294 (21)	196 (19)	210,[h] 235,[i] 245[j]
$D_r^{(1)} \times 10^{-3}$, s⁻¹	3.15 (0.38)	6.12 (0.64)	2.83 (0.26)	4.91 (0.50)	
$D_r^{(2)} \times 10^{-3}$, s⁻¹	*b*	6.15 (0.62)	*b*	5.04 (0.51)	
$D_r^{(3)} \times 10^{-3}$, s⁻¹	*c*	26.1 (7.3)	*c*	37.3 (11.0)	
τ_0, μs	52.9 (6.4)[e]	20.2 (2.5)[d]	58.9 (5.4)[e]	23.9 (2.7)[d]	38[i]
Rod					
$D^0_{20,w} \times 10^7$, cm² s⁻¹	1.41	1.43	1.33	1.34	1.24[h]
$[\eta]$, cm³ g⁻¹	290	181	355	271	265[j]
$D_r^{(1)} \times 10^{-3}$, s⁻¹	4.99	6.98	4.01	5.72	
$D_r^{(2)} \times 10^{-3}$, s⁻¹	*b*	7.89	*b*	6.22	
$D_r^{(3)} \times 10^{-3}$, s⁻¹	*c*	87.4	*c*	73.5	
τ_0, μs	33.4	15.6	4.16	19.4	24[k]

[a] Averages and standard deviations of values calculated for four or five different orientations of the head. [b] Equal to $D_r^{(1)}$. [c] Too large. [d] Equation 4. [e] Equation 5. [f] Herbert & Carlson (1971). [g] D'Albis & Gratzer (1976). [h] Lowey et al. (1969). [i] Rosser et al. (1978). [j] Burke & Harrington (1972). [k] Highsmith et al. (1977).

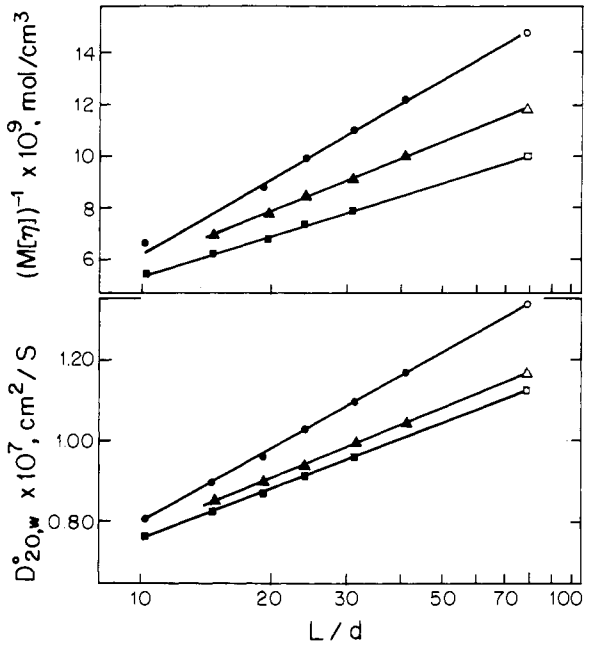

FIGURE 4: The same as in Figure 1 for the smallest and the largest rotational diffusion coefficients, $D_r^{(1)}$ and $D_r^{(3)}$. The coefficients $D_r^{(2)}$ are very close to those of $D_r^{(1)}$. Values are referred to water at 20 °C.

previous studies. Thus, Highsmith et al. (1977) and Sutoh et al. (1978) obtained L = 1440 Å, in agreement with the electron microscopy result of Takahashi (1978). Therefore, we took this value for the second set of lengths, and the bend was assumed to be at the middle.

The experimental value of the molecular weight is needed in order to transform the computer calculated values of $M_r[\eta]$ and $D^0_{20,w}$ to $[\eta]$ and $s^0_{20,w}$. Literature data for the molecular weight of myosin and its fragments show a remarkable scatter. A reasonable value for the rod is M_r = 250 000 (Highsmith et al., 1977). For myosin we have taken M_r = 470 000 which is close to 250 000 + (2 × 115 000) (rod plus two heads) and to other experimental results (Herbert & Carlson, 1971; Godfrey & Harrington, 1970).

As noted previously, the study of Elliot & Offer (1978) proposed that the heads are quite flexibly joined to the rod. Then, the observed properties must correspond to a conformational average over the angles θ_1,ϕ_1 and θ_2,ϕ_2. To take this flexibility into account, we calculated the hydrodynamic properties, with fixed L, L_1, and χ, for four or five randomly chosen sets of the head angles and obtained the mean value and standard deviation. The results for myosin and the rod are listed in Table I.

Our way of presenting the calculated rotational coefficients needs some further explanation. The computer programs calculate first the rotational diffusion tensor in the particle-fixed system of coordinates (Figure 2). Then this tensor is diagonalized to obtain its three eigenvalues, $D_r^{(1)}$, $D_r^{(2)}$, and $D_r^{(3)}$, where $D_r^{(1)}$ is the smallest and $D_r^{(3)}$ the largest. For χ = 90°, axis 2 is near the bisectrix of χ, axis 3 is perpendicular to axis 2 within the plane defined by the rod, and axis 1 is perpendicular to that plane. It is found that $D_r^{(1)}$ and $D_r^{(2)}$ are close to each other, as predicted in a previous study (García Bernal & García de la Torre, 1980), and $D_r^{(3)}$ is considerably larger. The decay of optical properties is a sum of several exponential terms (Wegener et al., 1979) whose corresponding relaxation times are complicated functions of $D_r^{(1)}$, $D_r^{(2)}$, and $D_r^{(3)}$. Nevertheless, the decay function may look like a single exponential within experimental error, with an experimental relaxation time τ_0. In fact, this is actually observed for the rod (Highsmith et al., 1977). Since the theory for the rotational decay of electrooptic properties of broken rods has not been developed yet, we tentatively equate the observed relaxation time to the mean of three relaxation times corresponding to each eigenvalue.

$$\tau_0 = [1/6D_r^{(1)} + 1/6D_r^{(2)} + 1/6D_r^{(3)}]/3 \quad (4)$$

Equation 4 also seems to be a logical choice for τ_0 when it is determined as the longest relaxation time in viscoelastic measurements (Rosser et al., 1978).

When χ = 180°, $D_r^{(3)}$ corresponds to rotation about the rod axis (z in Figure 2) while $D_r^{(1)}$ and $D_r^{(2)}$ are for rotation about perpendicular axes. Now, $D_r^{(1)} = D_r^{(2)}$ for the (straight) rod and this must also hold for myosin after averaging over the heads' orientation. $D_r^{(3)}$ is now very much larger than the two others, and its calculated value is meaningless because all the beads composing the rod lie on the rotation axis. The rotational diffusion will be therefore dominated, when χ = 180°, by the coefficient corresponding to rotation around a per-

Table II: Calculated and Experimental Hydrodynamic Properties of Heavy Meromyosin[a]

properties	calcd values L_1 = 720 Å	L_1 = 560 Å	L_1 = 430 Å	exptl values
$D^0_{20,w} \times 10^7$, $cm^2\ s^{-1}$	1.68 (0.04)	1.87 (0.06)	2.08 (0.08)	1.94[b]
$[\eta]$, $cm^3\ g^{-1}$	71.1 (8.6)	42.9 (5.8)	26.0 (4.1)	49[b]
$D_r^{(1)} \times 10^{-3}$, s^{-1}	17.4 (2.1)	31.1 (5.1)	55.5 (12.3)	
τ_0, μs	9.6 (1.1)[d]	5.4 (0.9)[d]	3.0 (0.7)[d]	5.0[c]

[a] See footnote *a* in Table I. [b] Lowey et al. (1969). [c] Kobayashi & Totsuka (1975). [d] Equation 5.

pendicular axis, so that it is reasonable to regard the relaxation time as

$$\tau_0 = 1/6D_r^{(1)} \quad (5)$$

Literature data for myosin and myosin rod, taken from the indicated references and normalized to 20 °C, are also included in Table I.

Heavy Meromyosin. Since the rodlike part in HMM is shorter than that in myosin, no extrapolations are necessary to reach the true axial ratio, and the properties can be calculated directly. As in the case of myosin, four or five conformations of the heads were randomly generated, and the resulting averages and standard deviations are given in Table II. Besides L_1 = 430 and 720 Å, an intermediate value, 560 Å, was also considered. The calculated values, along with experimental results, are listed in Table II. The same considerations about the rotational diffusion coefficients of myosin and myosin rod with $\chi = 180°$ apply here, so that Table II includes only $D_r^{(1)}$ and the relaxation times given by eq 4.

Discussion

Analysis of Theoretical Results. The data in Table I indicate that differences in the orientation of the heads produce quite small changes in the hydrodynamic properties of myosin. The standard deviations are nearly 1% of the average values for translational diffusion and ~10% for viscosity and the smaller rotational diffusion coefficients. In addition to that, the internal motion of the heads must be very weakly coupled to the overall translation and rotation of the particle as a whole (this will be discussed later in detail), and we therefore can conclude that the hydrodynamic properties of myosin examined in this paper are practically insensitive to the motion of the heads. This situation does not change appreciably for HMM, although the contribution from the heads is larger. A powerful tool for studying the head–rod hinge is nanosecond fluorescence anisotropy decay of head-labeled myosin (Mendelson et al., 1973), but the hydrodynamic description of this property is outside the scope of the present paper.

Table I shows that the calculated values of $D^0_{20,w}$ are also insensitive to variations in χ, while the rotational coefficient and $[\eta]$ show a strong χ dependence. This conclusion is in accord with previous studies on the hydrodynamics of broken rods (García de la Torre & Bloomfield, 1978; García Bernal & García de la Torre, 1980; Wilemski, 1977) and applies not only to the myosin rod but also to the myosin molecule as well. It is also noted in Tables I and II that viscosity and rotational diffusion are more sensitive to the length of the rodlike region than is translational diffusion, and this is a consequence of the fact that the two former properties depend on $L^3/\ln(L/D)$, while the latter varies as $L/\ln(L/d)$.

Flexibility Effects. The flexibility at the S-2–S-1 and S-2–LMM joints is presently regarded as responsible for the most important aspects of myosin function. It should be possible to detect this flexibility by using high-precision hydrodynamic techniques such as quasielastic light scattering and transient electric birefringence. Unfortunately, the hydrodynamic theory for hinged particles has not yet been fully developed. Some recent work in that direction has been done by Harvey (1978, 1979), who showed that noticeable changes in the diffusion coefficients are to be expected (with respect to the values for the corresponding rigid particle) when one part of the molecule moves relative to the rest of the molecule. These effects come from two different sources. First, flexibility allows the molecule to adopt a variety of conformations (different θ_1, ϕ_1, θ_2, ϕ_2, and χ angles in the case of our myosin models), each with different hydrodynamic properties. Then, at first glance, one can expect the observed properties to correspond to some ensemble (or time) conformational average. A simpler way of considering this would be to define, for each property, an average conformation for which the theory of rigid particles reproduces the corresponding observed value. In the case of myosin, we could obtain a χ for each property in this way.

The second effect of flexibility is the enhancement of *translational* diffusion due to its coupling with the internal motion (Harvey, 1979). However, this does not affect rotation, and the influence of viscosity must be small for low shear rates. Besides, the computed increase in translational diffusion, ~34% (Harvey, 1979), would perhaps be lowered if hydrodynamic interaction were completely taken into account. Therefore, we think that the flexibility analysis can be done, in a first-order approach, by using only the considerations described in the preceding paragraph. In addition, the internal motion of the heads is much less important than that of the rod, as seen in Table I. This is because the moving parts in this case make a small contribution to the hydrodynamic behavior of the whole particle, as can be easily concluded by comparison of myosin and rod values in Table I. Then, our procedure of averaging over randomly generated conformations of the heads seems to be well-founded. Thus, we are finally left only with the problem of flexibility within the rod.

Comparison with Experimental Results. Table I shows a remarkable disagreement between the experimental and calculated values of $D^0_{20,w}$. This is not surprising, however, because our calculation does not include the coupling effects described above. Also, the light-scattering value (Herbert & Carlson, 1971) could be vitiated by rotational contributions (Wilson & Bloomfield, 1979b), although this is unlikely at small scattering angles (F. D. Carlson, personal communication), while the result from $s^0_{20,w}$, M_r, and $\bar{v}$ should have an appreciable error owing to the accumulated experimental uncertainties in these three quantities. Nevertheless, translational diffusion is not the best property to examine when one is studying conformational changes or flexibility effects, as we have already pointed out.

It is seen in Table I that the experimental values of $[\eta]$ and τ_0 are well bracketed by those calculated for $\chi = 180°$ and $\chi = 90°$. This is so for myosin, and for the rod as well, regardless of the choice of L and L_1, and indicates that the χ's are higher than 90° but also substantially smaller than 180°. We believe that this is a definitive hydrodynamic proof of the flexibility of the rod and qualitatively agrees with the distribution of χ's observed in electron microscope images (Lowey et al., 1969; Elliot & Offer, 1978). We have not done a complete evaluation of the χ's because they will depend not only on the property measured but also on the choice of lengths. Besides, the accuracy of experimental data of $[\eta]$ and the uncertainty of our interpretation of the τ_0's do not guar-

antee the utility of further, time-consuming calculations. We can, at least, make such an analysis for the myosin rod with $L = 1440$ and $L_1 = 720$ (equal arms) by using our previous results for intrinsic viscosity (García de la Torre & Bloomfield, 1978) and rotational diffusion (García Bernal & García de la Torre, 1980) of broken rods. The experimental values of $[\eta]$ and τ_0 correspond, approximately, to $\chi_\eta = 135°$ and $\chi_\tau = 120°$.

We should note that several of the more recent experimental data used in Table I came from measurements made at low temperature (3–5 °C) to prevent aggregation, and we have converted them to 20 °C by means of a T/η_0 factor (absolute temperature over solvent viscosity) to make them compatible with other earlier results obtained at that temperature. However, this factor does not account for two other relevant temperature effects. First, if the S-2–LMM joint is not freely hinged but presents an elastic, restoring force (Harvey & Cheung, 1977), an increase in temperature will result in an increased flexibility. Second, and probably more important, partial melting can take place in the temperature range 0–20 °C, so that myosin would show more flexibility at 20 °C than at lower temperature. In other words, if those measurements could be made at 20 °C in a total absence of aggregates, the experimental values of D^0 would be higher and those of $[\eta]$ and τ_0 lower than those made at low temperatures and simply corrected with the T/η_0 factor. Then all these hypothetical experimental results at 20 °C would be farther from the theoretical results for $\chi = 180°$, reinforcing our conclusion about the flexibility within the rod.

It is impossible to ascertain which of the two sets of lengths in Table I fits best the observed properties, for it would require a rigorous evaluation of the contributions from flexibility. In the case of HMM, the hydrodynamic properties are mostly dominated by the length, L_1, assumed for subfragment S-2, as seen in Table II. Then, L_1 can be estimated by interpolation, the results being 510 Å from $D^0_{20,w}$, 580 Å from $[\eta]$, and 540 Å from τ_0. These values do not differ much from the hydrodynamic length of isolated subfragment S-2, 587 Å, as determined by Highsmith et al. (1977) using electric birefringence decay.

Acknowledgments

We are grateful to Professor F. D. Carlson for suggesting that we consider this problem and for comments on a preliminary version of the manuscript.

References

Broersma, S. (1960a) *J. Chem. Phys. 32*, 1632–1635.
Broersma, S. (1960b) *J. Chem. Phys. 32*, 1626–1631.
Burke, M., & Harrington, W. F. (1972) *Biochemistry 11*, 1456–1462.
D'Albis, A., & Gratzer, W. (1976) *J. Biol. Chem. 251*, 2825–2830.
Elliot, A., & Offer, B. (1978) *J. Mol. Biol. 123*, 505–519.
García Bernal, J. M., & García de la Torre, J. (1980) *Biopolymers 19*, 751–766.
García de la Torre, J., & Bloomfield, V. A. (1977a) *Biopolymers 16*, 1747–1763.
García de la Torre, J., & Bloomfield, V. A. (1977b) *Biopolymers 16*, 1765–1778.
García de la Torre, J., & Bloomfield, V. A. (1978) *Biopolymers 17*, 1605–1627.
Godfrey, J. E., & Harrington, W. F. (1970) *Biochemistry 9*, 894–908.
Harvey, S. C. (1978) *J. Chem. Phys. 69*, 3426–3427.
Harvey, S. C. (1979) *Biopolymers 18*, 1081–1104.
Harvey, S. C., & Cheung, H. C. (1977) *Biochemistry 16*, 5181–5187.
Herbert, T. J., & Carlson, F. D. (1971) *Biopolymers 10*, 2231–2252.
Highsmith, S., Kretzschmar, K. M., O'Konski, C. T., & Morales, M. F. (1977) *Proc. Natl. Acad. Sci. U.S.A. 74*, 4986–4990.
Huxley, H. E. (1969) *Science (Washington, D.C.) 164*, 1356–1366.
Kobayashi, S., & Totsuka, T. (1975) *Biochim. Biophys. Acta 376*, 375–385.
Kretzschmar, K. M., Mendelson, R. A., & Morales, F. (1978) *Biochemistry 17*, 2314–2318.
Lowey, I., Slayter, H. S., Weeds, A. G., & Baker, H. (1969) *J. Mol. Biol. 42*, 1–29.
Lowey, S. (1971) *Biol. Macromol. 5*, 201–259.
Mendelson, R. A., Morales, M. F., & Botts, J. (1973) *Biochemistry 12*, 2250–2255.
Miller, A., & Tregear, R. T. (1972) *J. Mol. Biol. 70*, 85–104.
Moore, P. B., Huxley, H. E., & De Rosier, D. J. (1970) *J. Mol. Biol. 50*, 279–295.
Nakajima, H., & Wada, Y. (1977) *Biopolymers 16*, 878–893.
Rosser, R. W., Nestler, F. H. M., Schrag, J. L., & Ferry, J. D. (1978) *Macromolecules 11*, 1239–1242.
Sutoh, K., Sutoh, K., Karr, T., & Harrington, W. F. (1978) *J. Mol. Biol. 126*, 1–22.
Takahashi, K. (1978) *J. Biochem. (Tokyo) 83*, 905–908.
Tirado, M. M., & García de la Torre, J. (1979) *J. Chem. Phys. 71*, 2581–2587.
Tsuda, K. (1970) *Polym. J. 1*, 616–631.
Wegener, W. A., Dowben, R. M., & Koester, J. T. (1979) *J. Chem. Phys. 70*, 622–632.
Wilemski, G. (1977) *Macromolecules 10*, 28–34.
Wilson, R. W., & Bloomfield, V. A. (1979a) *Biopolymers 18*, 1205–1211.
Wilson, R. W., & Bloomfield, V. A. (1979b) *Biopolymers 18*, 1435–1549.
Yamakawa, H., & Fujii, M. (1973) *Macromolecules 6*, 407–412.
Yang, J. T., & Wu, C. C. (1977) *Biochemistry 16*, 5785–5789.
Yoshizaki, T., & Yamakawa, H. (1980) *J. Chem. Phys. 72*, 57–69.